

Predicting the Behavior of Screen Printing

Nikil Kapur, Steven J. Abbott, Elisabeth D. Dolden, and Philip H. Gaskell

Abstract—A novel mathematical model is presented of the liquid transfer process encountered during screen printing, enabling the prediction of the volume of liquid removed from a mesh and printed on a substrate with reasonable accuracy. It is based on the key assumption that free surface effects dominate and the printed liquid is pulled out of, rather than flows from, the mesh. The model is validated against an extensive range of benchmark data from both on- and off-screen printing trials. The agreement is found to be remarkably good. In addition, the model is able to offer considerable insight to practitioners and liquid manufacturers alike—a key result being that the screen printing process can be made essentially independent of many of the set-up parameters in the operating range adopted by most practitioners.

Index Terms—Liquid transfer, mathematical modeling, screen printing.

I. INTRODUCTION

UNDERSTANDING the science of screen printing has been less than satisfactory, despite its widespread use—traditionally in the field of graphics. However, it has seen growth in manufacturing processes such as large area electronics [1] and organic electronics [2] with potential for printing over large areas on relatively cheap substrates [3], and in applications such as multilayer solar cell manufacturing [4]. Advances have been made, particularly in how the mesh forming the screen is filled with liquid, but insight into the key aspect of how the liquid is subsequently transferred from the screen to the substrate are almost nonexistent. Ironically, it is control of the latter that is of prime importance since it governs the performance characteristics of the process.

In what appears to be the first of a series of papers by Riemer, spanning over two decades, directed at analytically modeling the screen printing process, he concluded [5] that transfer of liquid from the screen to the substrate was attributable entirely to the forces of adhesion. He soon modified this view, however, after diverting his attention to the role of the squeegee blade in the process [6]–[10]. Other researchers [11]–[15] have similarly investigated the action of the squeegee blade in filling the screen, using computational fluid dynamics

(CFD) simulations [16], among others. In all cases, the film profile under the blade tip was taken as fixed and the squeegee itself assumed perfectly rigid, although recently this latter condition has been relaxed [17] and more realistic boundary conditions have been included on the free surface [18]. While these works tell us much about the hydrodynamic conditions that exist at the squeegee tip, a less than convincing argument has emerged as to the role played by associated pressure differentials in the screen-to-substrate transfer process. The same is true of the studies based on lubrication theory which treat the screen as a permeable membrane—or region of interconnected capillaries—invoking Darcy’s law to make the problem tractable analytically, see [19]–[21]. Furthermore, the combined body of work in [5]–[21] does not offer predictions of actual deposited film, which is a key requirement of the screen printing industry.

On reflection, none of the above researchers appears to have addressed the fundamental underlying assumption inherent in their work, namely, that the action of the squeegee in filling the screen is coupled to the subsequent emptying process. Messerschmitt [22], on the other hand, offered a different perspective. He explored the idealized problem of the emptying of a single mesh opening, arguing that the surface tension of the liquid played an important role in the process, in that it controlled the evolution of the liquid bridge-like structure [23] that evolves as the screen and substrate separate. He described four key stages of the transfer of the ink to the substrate: adhesion, extension, flow, and separation. Consequently, he made a number of key observations concerning the screen-to-substrate transfer, the significance of which remained largely unrecognized in the intervening years.

The first of these is that, if adhesion were significant, then the bulk of the liquid would tend to remain on the screen and not be transferred to the substrate, counter to what is observed in practice. Second, he concluded that pressure differentials generated by the squeegee play no role in screen-to-substrate liquid transfer since they have no effect once the transfer begins. Third, gravity and the presence of air above the screen have a negligible effect on the process since it is possible to screen print both against gravity and in a vacuum.

The mechanism that is consistent with these observations is shown in Fig. 1; the key to understanding screen printing is to break it down into a series of constituent elements. In Fig. 1, a 2-D representation of the mesh is used: the fibers are shown in cross-section in just one of the two weave directions. For traditional off-contact printing (as this is the more commonly used mode of operation), the first pass of the blade (the flood stroke) spreads an excess of ink on top of the mesh [Fig. 1(a)]. The second stage is where the blade passes again (the print stroke), causing the mesh to be forced

Manuscript received June 14, 2012; revised September 7, 2012; accepted October 15, 2012. Date of publication January 9, 2013; date of current version February 21, 2013. Recommended for publication by Associate Editor W. D. Brown upon evaluation of reviewers’ comments.

N. Kapur and P. H. Gaskell are with the School of Mechanical Engineering, University of Leeds, Leeds LS2 9JT, U.K. (e-mail: n.kapur@leeds.ac.uk; p.h.gaskell@leeds.ac.uk).

S. J. Abbott is with MacDermid Autotype Ltd, Wantage OX12 7BZ, U.K. (e-mail: steven@stevenabbott.co.uk).

E. D. Dolden is with Sharp Laboratories of Europe Ltd., Oxford Science Park, Oxford, OX4 4GB, U.K. (e-mail: elisabeth.dolden@sharp.co.uk).

Color versions of one or more of the figures in this paper are available online at <http://ieeexplore.ieee.org>.

Digital Object Identifier 10.1109/TCPMT.2012.2228743

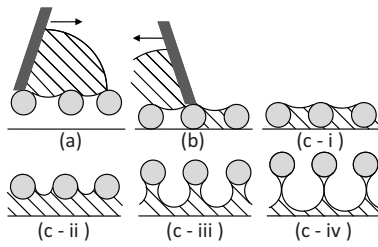


Fig. 1. Schematic showing the three stages of screen printing. (a) Excess of fluid on mesh after flood stroke. (b) Squeegee forces screen into contact with substrate and fills cavities with ink. (c) (i-iv) Screen separates from substrate and ink is pulled from mesh.

into contact with the substrate and at the same time filling the mesh with ink [Fig. 1(b)]. The final stage occurs when the tensioned mesh lifts from the substrate and ink is drawn from the mesh in a series of liquid-bridge-type structures [Fig. 1(c) (i-iv)]. The squeegee plays no part in this since a simple geometric argument shows it is now many threads away from the print-forming zone. Ultimately these bridges break, giving the print on the substrate and leaving the residual ink on the mesh. This figure can be interpreted in terms of the four stages identified by Messerschmitt [22]: adhesion [Fig. 1(c) (i)], extension (Fig. 1(c) (ii)), flowing (Fig. 1(c) (iii)), and separation (Fig. 1(c) (iv)). A key development shown in Fig. 1 over that in [22] is the inclusion of multiple threads and the corresponding change this makes to the flow path.

Here we present, for the first time, a mathematical model capable of predicting the volume of liquid transferred from the screen to the substrate during screen printing. The experimental arrangement is described in Section II. The analytical model is formulated in Section III, the key feature of which is that liquid is assumed to be pulled out of rather than flow from the screen, forming a liquid bridge, as the free surface conforms to preserve the volume. In Section IV, the results are presented and validated against extensive experimental data taken from here and also those provided by Hohl [24] of the Screen Printing Technical Foundation (SPTF). These compare well over a wide range of screen mesh densities. Next, in Section V, a discussion of the limitations and practical implications of the model are discussed, followed by concluding remarks in Section VI.

II. EXPERIMENTAL APPARATUS AND METHOD

The on-contact experiments were carried out on a small screen printing rig, which was designed to enable control between the printing stages discussed in the introduction. Fig. 2 shows a schematic diagram of the rig, which consists of a support frame on which is attached the mesh at an angle of 0.8° to the vacuum platform, which helps assist snap-off. The mesh used in this study is a Saati 90-40 OU-PW. Applied to this was a stencil of 0.17×0.17 m open area with a centrally located 0.01×0.01 m blocked area. This was used to check the print quality by examining the resolution of the edges of this area. A variable speed motor was used to raise and lower the substrate in the range $1-25$ mms^{-1} .

The inks investigated in the on-contact experiments were the Sericol Seridisc trichromatic set and an additional ink

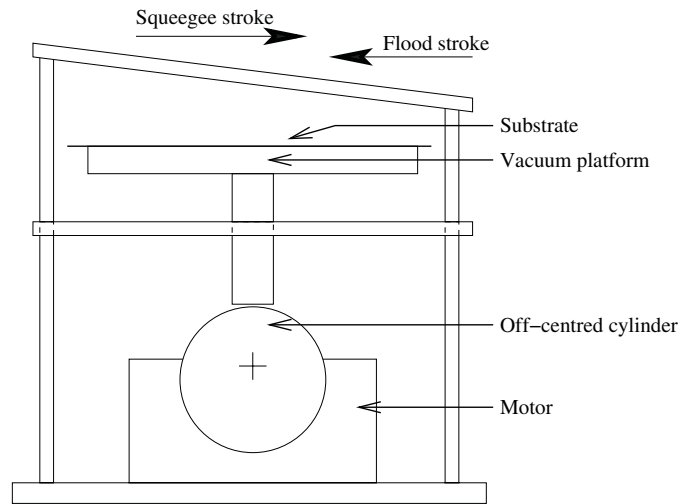


Fig. 2. Schematic of the experimental apparatus.

TABLE I
DENSITIES OF THE INKS USED IN THE EXPERIMENTS

Ink	Density (kgm^{-3})
Sericol black	1245
Sericol cyan	1226
Sericol magenta	1214
Sericol yellow	1258
Sericol white	1432
Nazdar black	1047

Sericol UViplast Opaque White. The density of each ink was measured by filling a cup of known volume and scrapping off the excess ink before weighing; the values are given in Table I. The viscosity of the inks was measured using a cone and plate geometry on a Bohlin rheometer; the results are shown in Fig. 3.

To obtain a print, the following series of steps were followed: 1) the substrate was positioned on the vacuum platform, and raised so that it was in intimate contact with the mesh; 2) an excess of ink was spread onto the mesh; 3) this was then metered using a squeegee stroke; and 4) the substrate was lowered at the desired motor speed so that the substrate separated from the mesh and printing occurred. Initial prints were discarded until good quality was obtained when the mesh became satisfactorily prewetted. The mass of ink transferred to the substrate was calculated by measuring the difference between the substrate directly before and after printing (with no curing). From this, the average film thickness for each print, h_{av} , was calculated using

$$h_{av} = \frac{m_{\text{ink}}}{\rho_{\text{ink}} A_{\text{print}}} \quad (1)$$

where m_{ink} is measured through the difference in mass of the substrate before and after printing, ρ_{ink} is the density of the ink (Table I), and A_{print} is the area of the print.

Tests carried out at McDermid Autotype show that amount of ink printed on a conventional press was identical to that from this test press.

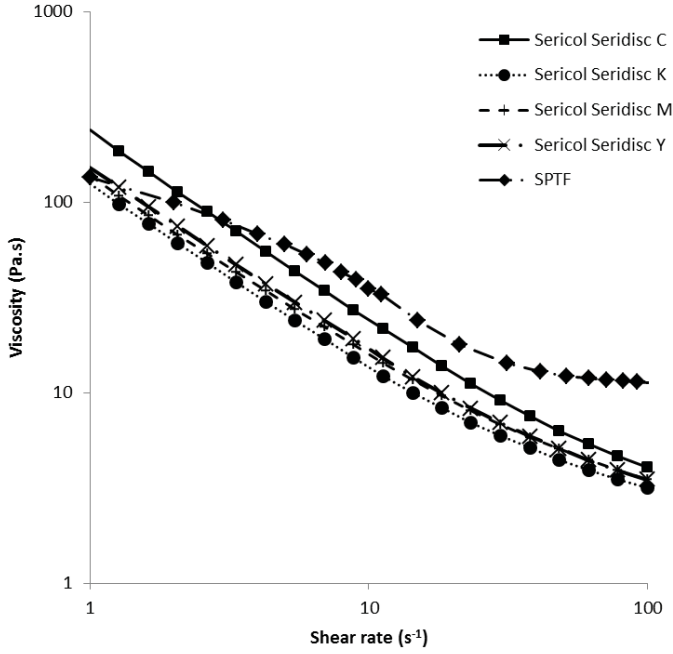


Fig. 3. Flow curve (viscosity dependence on shear rate) of the inks used in this paper and the SPTF study.

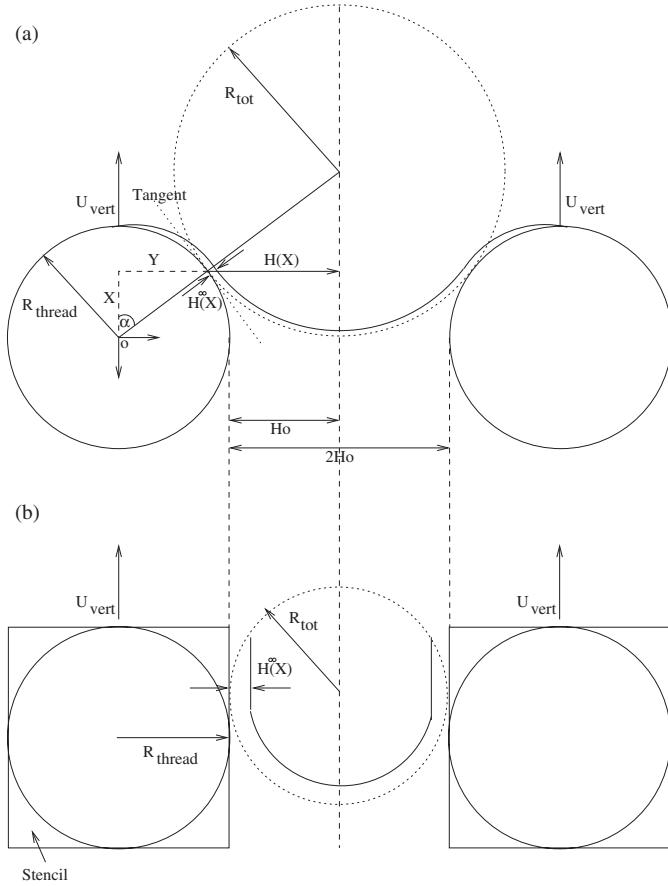


Fig. 4. Geometry of (a) 2-D mesh and (b) stencilled portion of the mesh with a single opening.

III. MATHEMATICAL MODEL

In order to simplify what is clearly a complex topological problem involving the infiltration of a free surface through a

3-D structure, the flow is considered in 2-D only. The threads making up the screen are assumed to be cylindrical and of radius R_{thread} , separated by a minimum distance of $2H_0$, and lie parallel to the squeegee blade and perpendicular to the direction of motion of the squeegee. Fig. 4 represents a cross-sectional plane through the threads, giving a schematic illustration of the transfer process for a unit cell as the screen and the substrate separate. Since the unit cell is symmetric about its vertical center line, periodic boundary conditions exist to the left and right. The challenge, therefore, is to formulate a means of predicting the residual liquid film left on the screen once the liquid bridge attached to each individual thread has broken, and hence the amount of liquid transferred to the substrate. The model is based on the following simplifying assumptions.

- 1) The liquid is incompressible, body forces are negligible, and no-slip boundary conditions exist at the surfaces of the substrate and screen. Inertial effects are also negligible because of the modest speeds and small length scales involved in screen printing; the associated Reynolds number < 1 .
- 2) The tip of the squeegee blade is sharp and rigid, and its action: a) fills the screen by forcing liquid into it; b) on passing over the mesh leaves the liquid level and parallel with the top of the screen; and c) has nothing at all to do with the subsequent transfer of liquid to the substrate. These restrictions are relaxed and discussed later in this paper.
- 3) The tension of the screen is only considered in its role of keeping the screen straight between the frame to which it is fixed and the point where the squeegee presses it in contact with the substrate.
- 4) The shape of the free surface as it infiltrates the screen follows that of its radius of curvature; it conforms to preserve volume with the transfer of liquid being thought of as a series of quasi-steady steps; splitting (total separation) occurs when adjacent free surfaces meet beneath the thread.

Fig. 4 shows the coordinate system used to formulate the problem. Note that the radius of curvature of the free surface and its speed vary according to its location as a screen unit cell lifts away from the substrate. The problem can thus be broken down into two stages.

- 1) For each value of X , the radius of curvature of the free surface $R_{\text{men}}(X)$ and its speed $U_{\text{men}}(X)$ need to be calculated. It is then necessary to relate these to the residual film thickness remaining on the mesh.
- 2) Determination of whether adjacent free surfaces have touched satisfying the condition for total separation and calculation of the transfer fraction.

To calculate the residual film thickness, the following methodology is adopted. With reference to Fig. 5, the half-gap $H(X)$, at any location X is given by

$$H(X) = H_0 + R_{\text{thread}} - \sqrt{R_{\text{thread}}^2 - X^2} \quad (2)$$

where the minimum gap is related to the more usual mesh description of threads per unit length, and thread diameter through $H_0 = (1/M) - (D_{\text{thread}}/2)$. Typically M is reported

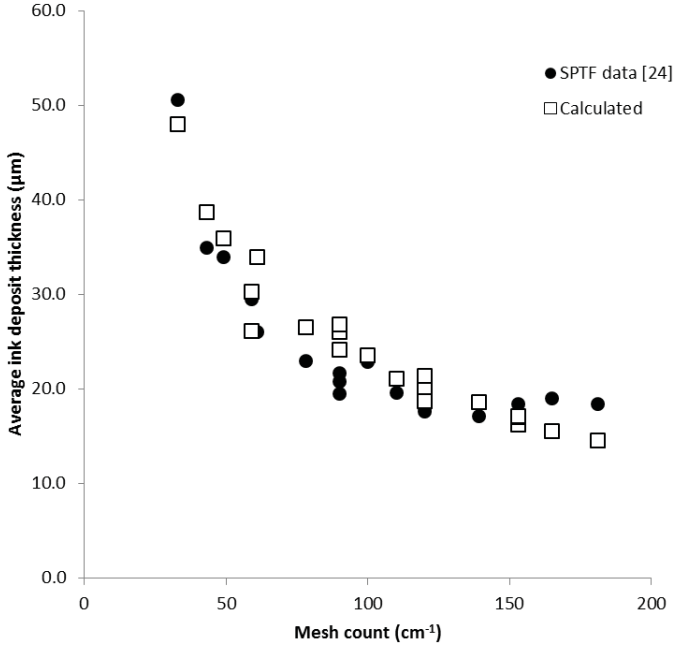


Fig. 5. Comparison of the model predictions with the SPTF dataset. Note multiple points at one screen density relate to different thread diameters.

in cm^{-1} and D_{thread} in micrometers, in which case $H_0 = (1/100M) - (D_{\text{thread}}/2 \times 10^6)$ in meters.

The gradient of the tangent to the thread by

$$\frac{dY}{dX} = -\frac{X}{\sqrt{R_{\text{thread}}^2 - X^2}}. \quad (3)$$

The radius R_{tot} defined as

$$R_{\text{tot}} = H^\infty(X) + R_{\text{men}} \quad (4)$$

which can be calculated by matching the tangent of this to the tangent of the thread to give

$$R_{\text{tot}} = H(X) \left(1 + \left(\frac{dY}{dX} \right)^2 \right)^{1/2} \quad (5)$$

where $H^\infty(X)$ is the thickness of the film, measured in the radial direction, remaining on the thread.

The speed of the meniscus now needs to be related to the residual film thickness on the mesh. To do this, recourse is made to associated work concerning the prediction of the film thickness $H^\infty(X)$ of a liquid layer attached to substrate which is pulled from a liquid as a function of the capillary number $Ca_{\text{men}} = \mu U_{\text{men}}/\sigma$, where μ and σ are the viscosity and the surface tension of the fluid, respectively, with Ca_{men} a measure of the ratio of viscous forces to surface tension forces. The relationship between the residual film thickness and the radius of curvature of the meniscus can be written in general form, as derived analytically by Landau and Levich [25]

$$\frac{H^\infty}{R_{\text{men}}} = aCa_{\text{men}}^b. \quad (6)$$

The constant coefficients in (6) have been evaluated analytically [25]–[28] for small capillary numbers. Fairbrother and Stubbs [29], and Taylor [30] suggested similar values

for these coefficients from experiments involving a capillary tube and flow between parallel plates, respectively. Taylor [30] extended the range of this relationship, and, for higher capillary numbers, Ruschak [31], [32] fitted it to data from a finite-element simulation of forward roll coating and data taken from a similar analytic study by Coyne and Elrod [33]. Note that the data has from Ruschak has been reinterpreted in terms of H^∞/R_{men} rather than H^∞/H_0 as given in his papers.

The values of the associated coefficient and the limits over which they apply are as follows:

$$a = 1.34, \quad b = 0.66; \quad Ca < 0.023, \quad [25]$$

$$a = 0.50, \quad b = 0.4; \quad 0.023 < Ca < 2, \quad [30]$$

$$a = 0.66, \quad b = 0; \quad 2 < Ca. \quad [31], [32].$$

The range most appropriate for this paper is the last, since the capillary number involved in screen printing (based on a typical viscosity of order 10 Pa.s, surface tension of 0.03 Nm^{-1} , and conservative snap-off speed of 2 mm^{-1}) is of order $Ca = 10$. Here, the film thickness remaining on the threads behind the advancing meniscus is independent of the fluid properties and (6) reduces to $H^\infty/R_{\text{men}} = \text{const}$.

All that remains now is to evaluate the residual film. Combining (4) and (6) enables this to be calculated using

$$H^\infty(X) = \frac{R_{\text{tot}} a C a_{\text{men}}^b}{1 + a C a_{\text{men}}^b} \quad (7)$$

and under the conditions of high capillary number this reduces to

$$H^\infty(X) = 0.4 R_{\text{tot}}. \quad (8)$$

The volume remaining on the thread can be calculated using numerical integration between the top of the thread and the point when the two menisci moving round a given thread intersect. The model is concerned solely with modeling the ink around the thread, and does not describe the pattern of deposition on the substrate, in particular when the free surface is located near the bottom of the thread the radius of curvature intersects the substrate. Despite this, the fraction ϕ of liquid transferred to the substrate ϕ can be determined by considering the difference between the initial volume of ink contained within the 2-D idealized mesh associated with one thread, given by $V_i = 4R_{\text{thread}}^2 - \pi R_{\text{thread}}^2$. The final volume of ink as a result of the integration process described above is

$$\phi = \frac{V_i - V_{\text{final}}}{V_i}. \quad (9)$$

The (theoretical) maximum printed thickness where all fluid is transferred to the substrate, H_{max} , from the 3-D mesh is given by [15]

$$H_{\text{max}} = 2R_{\text{thread}} \left(2 - \pi R_{\text{thread}} M \sqrt{1 + (2R_{\text{thread}} M)^2} \right). \quad (10)$$

Alternate expressions have been developed that incorporate additional geometric details [33], but these do not change the underlying description of the process. Accordingly, the actual printed thickness H_{act} can be inferred by scaling the maximum film thickness given above with ϕ obtained from the associated 2-D calculation

$$H_{\text{act}} = \phi H_{\text{max}}. \quad (11)$$

There are two regions where the model can lead to nonphysical predictions. At the top of a thread—where R_{tot} is big—the model predicts a large film thickness due to the over simplification of the meniscus geometry. However, the radial film thickness is restricted to that of the starting conditions. Similarly, when the meniscus is close to the bottom of a thread, the lower part of it intersects the substrate. Since we are not interested in the exact distribution of liquid on the substrate but only the transferred fraction, this does not affect the calculation procedure. Modifying the meniscus shape, by allowing it to move laterally as its path is blocked by the substrate, rather than relying on intrinsic geometry, does not affect the calculated liquid deposit, but does provide a more realistic picture of the process.

By slightly varying the geometry of the model, as illustrated in Fig. 4(b), the effect of an idealized stencil or the use of a square edged mesh can be incorporated in the calculations. The calculation procedure outlined above remains the same, although the radius and speed of the meniscus are now constant, as the free surface travels through the stencilled part of the mesh.

IV. RESULTS

A. Comparison With SPTF Data

A considerable challenge for any model is its ability to predict liquid deposits as compared to an industry benchmark dataset. Here, we use the extensive data associated with the printing of ink, collected by the SPTF. Fig. 5 shows a graph of printed film thickness as a function of the mesh count. The relevant operating variables were taken from the SPTF experiments and are as follows: 1.8 mm snap-off; 8 mm s^{-1} print speed; 0.45 m mesh length; surface tension 0.025 Nm^{-1} ; and non Newtonian properties as shown in Fig. 3. The multiple points shown at some mesh counts are for different thread diameters.

Although the agreement is not perfect, given the experimental difficulties in obtaining such a dataset over a wide range of meshes, the fit is reasonably good. The dataset illustrates the relationship between the fraction of the ink contained within the mesh and the printed thickness; as the mesh count is doubled from 90 to 180 cm^{-1} , the maximum printable thickness decreases by 50% but the printed ink thickness decreases by only 30%. This is equivalent to a greater proportion of ink being transferred from a fine mesh than from a coarse mesh.

B. Comparison With Our Data

Fig. 6 show the results of printing the Sericol ink range for the mesh at different peel-off rates. The first observation that can be drawn from this figure is that the printed film thickness is not affected by the peel-off rate, which suggests that the process is operating where H^∞/R_{men} is independent of the meniscus speed, i.e., in the high capillary region. There is a mild dependence of the printed ink thickness on fluid properties, which may be due to a fractional filling of the mesh where the squeegee removes the ink to some depth below the

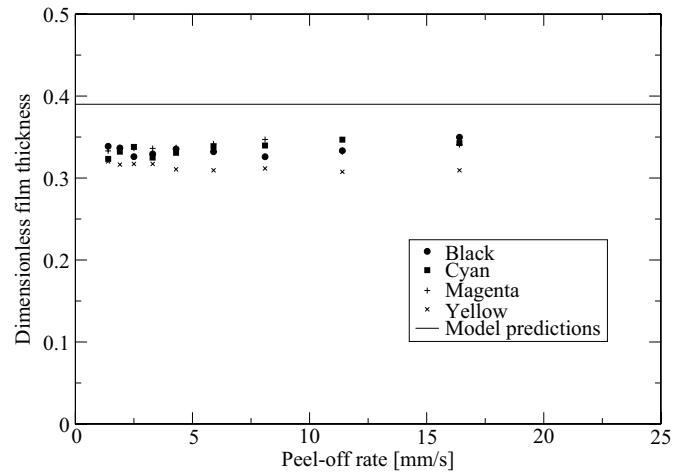


Fig. 6. Comparison of the model predictions with the results from the on-contact screen printing experiments.

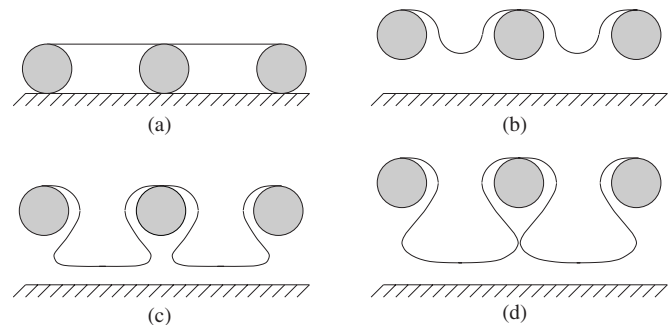


Fig. 7. Profile of the free surface when printing through an open mesh area showing (a) mesh in contact with substrate, (b) and (c) evolution of the meniscus through the mesh and (d) snap-off of the mesh and substrate.

maximum thickness of the web. Fig. 10 shows an image taken from the on-contact experiments illustrating this.

Included on Fig. 6 is the measured and predicted film thickness from the ink transfer model described in Section III. The model over estimates the printed film thickness of the experimental results by typically 10–15%.

The data in Sections IV-A and B illustrates a very important point—that the fraction of ink remaining on the screen (both measured experimentally and captured with the analytical model) is typically between 20% and 40% of the ink that initially fills the screen, with the remainder of the ink being transferred to the print. Section IV-E describes the controlling parameters in more detail.

C. Evolution of the Meniscus

Fig. 7 shows the evolution of the meniscus as it infiltrates the mesh as predicted by the model. There are four distinct stages: 1) the mesh is full and the squeegee has just passed by; 2) the gap between the screen and substrate has increased and, as the meniscus passes through the mesh, it leaves a residual film behind; 3) the shape of meniscus is now controlled by the mesh and the substrate; and 4) two menisci meet in a neck and the separation between screen and substrate is complete. The physics of the breakup is more complex than that suggested

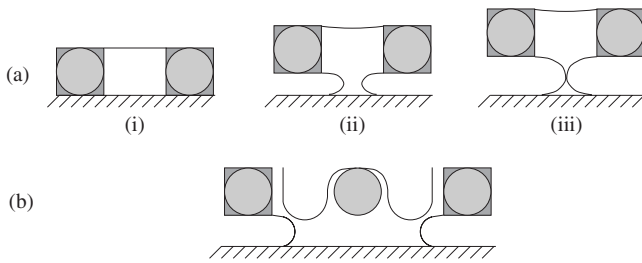


Fig. 8. Profile of the free surface when printing through a stencilled portion of the mesh with (a) single opening and (b) two openings.

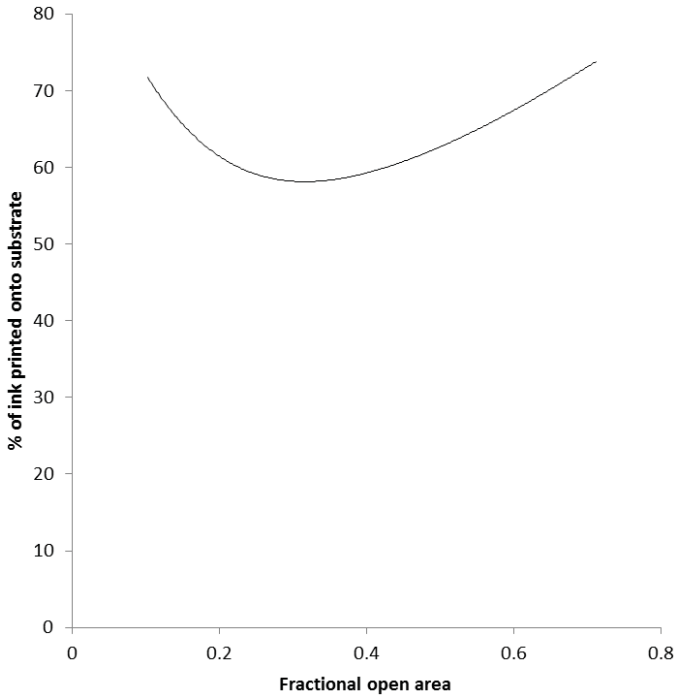


Fig. 9. Predicted transfer of fluid to the substrate at high Ca (>10) as a function of the open fraction of the mesh.

here: for example, it is well known that such necks are unstable and often, as they break, form a satellite droplet [23], which may explain the phenomenon of ink splatter. With elastic fluids, the necks can be more stable and stretch into long filaments, which may be why some screen printing inks have been observed to form strings.

D. Effect of Square-Edged Meshes or Stencils

Fig. 8(a) shows a schematic of the transfer of liquid through either a square-edged mesh (such as a nickel mesh) or a stencil with a single hole of the size of the mesh. The lower meniscus is pinned by the edge of the flow opening and, as the center of the meniscus moves toward the middle, it leaves almost no fluid on the substrate. This agrees with the common observation that it is impossible to print out of single holes. Efforts to round off square-edged meshes will improve print definition.

Fig. 8(b) shows the transfer of liquid out of a stencil where the hole consists of two mesh openings. More fluid can be printed out of this arrangement than with single mesh opening, but still less than without any stencil.

The results also indicate that other effects are important. For example, a stencil reduces the starting volume by filling the space above the middle of the threads (except in cases where the thickness of the stencil is very large). This reduction in volume, as well as the change in fraction of fluid transferred to the substrate, could provide one possible explanation for the classic dot-gain curve.

E. Effect of Thread Count and Diameter

Under typical printing conditions of $Ca > 2$, the fluid properties have little effect on the final print thickness. Instead, the thread count and diameter dictate the fraction of ink transferred to the mesh. These parameters can be encompassed in one nondimensional grouping given by the open fraction F_{open} of the mesh, which is simply defined as

$$F_{\text{open}} = 1 - MD_{\text{thread}} \times 10^{-4} \quad (12)$$

where M is in threads per cm and D_{thread} is in microns.

Fig. 9 shows that, as the open fraction of the mesh is increased, the fraction of ink remaining on the threads decreases. It should be remembered that as either M or R_{thread} is varied, the maximum print thickness calculated from (12) will also vary, and the final film thickness is a product of the percentage of ink transferred to the substrate read from the graph and the maximum film thickness from (12). By capturing all the behavior of the printing process in Fig. 9, it is no longer necessary to have to resort to the mathematical model described in Section III to calculate the final print thickness.

V. DISCUSSION

Whilst the model captures the principal dependence of film thickness on mesh geometry, it does not incorporate all physical interactions taking place during printing. In addition, there is variation in print thickness across the range of inks which are not explained by simple shear rheology measurements. This suggests that additional factors play a role in determining the final print thickness. Two particular areas that may yield further insights into the process are 1) a more detailed analysis of the effect of ink rheology, including the role of elasticity and yield stress, and 2) the interaction of the flexible blade with the mesh during the print stroke. Visualizations of the mesh just prior to snap-off [33] using the on-contact screen rig (Section II) suggest that the mesh is not necessarily full at this point, and the fluid level starts at some depth below the top of the mesh (Fig. 10). This reduces the volume of ink available during the print step. This, and the simplification of the mesh volume (10), may account for the differences between the model predictions and experimental results. Mesh tension is unlikely to affect the transfer. For most normal conditions, the assumption that the screen does not bow is adequate, so mesh tension should have no effect on liquid deposit. Exceptions are when the mesh is sagging under very low tensions, and when the squeegee is near the ends of the mesh where the distortions are greatest; a good setup will avoid both.



Fig. 10. Top view of the mesh during on-contact screen printing after the fill stroke and prior to snap-off.

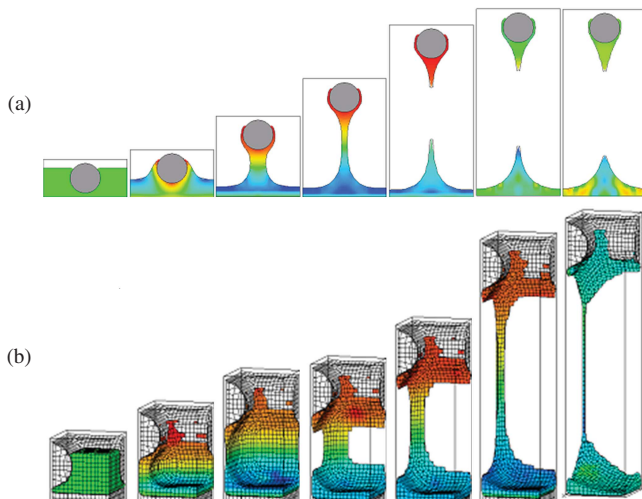


Fig. 11. Computational fluid mechanics simulations of the mesh separating from the substrate showing (a) 2-D, and (b) 3-D models where the mesh is represented as interlocking cylinders. This supports the underpinning mechanism described in this paper.

The interaction of this deformable squeegee and the substrate has formed the basis for much of the existing work described in the literature. Whilst the traditional held view is that ink is forced through the mesh, the model described in this paper separates out the filling of the mesh (driven by the pressure generated at the blade tip) and the snap-off of the mesh from the substrate (the print step). It may therefore be possible to relate the volume of fluid within the screen at the start of the print stroke using an existing analytical or computational model [5]–[21] and couple this with the model for the print step described here.

Finally, whilst the focus of this paper has been to develop a phenomenological understanding and underpinning analytical model, we note that the results from CFD [34], where the underlying Navier–Stokes equations describing fluid flow together with boundary conditions to represent the free surface, support the mechanism described here. A series of images are shown in Fig. 11, for both 2-D and 3-D mesh geometries, separating from the substrate. Whilst the analytical model predicts mean film thickness predictions, the CFD study can also give information about the topography of the printed film; evident from Fig. 11 is the tendency of the print to be thicker (as observed in [4]) beneath the knuckles of the web

rather than, as commonly supposed, beneath the open areas of the mesh. The surface tension and rheological characteristics of the fluid, together with the drying rate, will affect the subsequent leveling of such films.

VI. CONCLUSION

A strikingly simple and novel model of a complex topological problem was presented that revealed a wealth of detail about the screen printing process, in particular the liquid transfer mechanism. This understanding is fundamental if the process is to be developed to meet the demands of future hi-tech markets. It also provided, for the first time, a means of predicting with reasonable accuracy the volume of liquid deposited from a screen as a function of the mesh count. Indeed, agreement between theory and experiments for both on- and off-screen printing was very good over a wide range of mesh counts.

We now know from the model why it is possible to screen-print in a controlled way at all. The key feature is that the capillary number effect asymptotes in the regime where most printers tend to operate, leading to independence of the process on many of the set-up parameters.

ACKNOWLEDGMENT

The authors would like to thank the SPTF, in particular D. Hohl, for their generosity in providing access to the full dataset from their major study. They would also like to thank their colleagues in the screen-print industry for their willingness to listen to the theory and to engage in constructive debate. The theory described in this paper has been encapsulated in a user-friendly visual modeler which, in addition to calculated data, provides an evolving image of the screen printing process—the graphics are drawn to scale so that the relevant aspects (mesh spacing, separation, etc.) can be viewed in correct proportion. A copy of the associated software is available from Prof. S. J. Abbott (steven@stevenabbott.co.uk); it was developed at MacDermid Autotype, and a practical guide to screen printing (*How to be a Great Screen Printer*) based on these theories is available from the MacDermid Autotype website.

REFERENCES

- [1] R. Parashkov, E. Becker, T. Riedl, H.-H. Johannes, and W. Kowalsky, "Large area electronics using printing methods," *Proc. IEEE*, vol. 93, no. 7, pp. 1321–1329, Jul. 2005.
- [2] C. H. Chason, P. W. Brazis, J. Zhang, K. Kalyanasundaram, and D. R. Gamota, "Printed organic semiconducting devices," *Proc. IEEE*, vol. 93, no. 7, pp. 1348–1356, Jul. 2005.
- [3] P. A. Parashkov, E. Becker, T. Riedl, H.-H. Johannes, and W. Kowalsky, "Large area electronics using printing methods," *Proc. IEEE*, vol. 93, no. 7, pp. 1321–1329, Jul. 2005.
- [4] K. R. Krebs, M. Jorgensen, K. Norrman, O. Hagemann, J. Alstrup, T. D. Nielsen, J. Fyenbo, K. Larsen, and J. Kristensen, "A complete process for production of flexible large area polymer solar cells entirely using screen printing—first public demonstration," *Solar Energy Mater. Solar Cells*, vol. 93, no. 4, pp. 422–441, 2009.
- [5] D. E. Riemer, "The direct emulsion screen as a tool for high resolution thick film printing," in *Proc. Electron. Compon. Conf.*, 1971, pp. 463–467.
- [6] D. E. Riemer, "Ink hydrodynamics of screen printing," in *Proc. Ink Hydrodynam. Screen Print. Conf.*, 1985, pp. 52–58.

- [7] D. E. Riemer, "The function and performance of the stainless steel screen during the screen-print ink transfer process," in *Proc. Int. Symp. Microelectron. Symp.*, 1986, pp. 826–831.
- [8] D. E. Riemer, "The shear and flow experience of ink during screen printing," in *Proc. Ink Hydrodynam. Screen Print. Conf.*, 1987, pp. 335–340.
- [9] D. E. Riemer, "Analytical engineering model of the screen printing process: Part I," *Solid State Technol.*, vol. 1, pp. 107–111, May 1988.
- [10] D. E. Riemer, "Analytical engineering model of the screen printing process: Part II," *Solid State Technol.*, vol. 1, pp. 85–90, May 1988.
- [11] D. O. Brown, "Screen printing—an integrated system," in *Proc. Int. Symp. Microelectron. Conf.*, 1986, pp. 582–590.
- [12] P. K. Ajmera, B. Huner, and H. Rangchi, "A model for deposition of thick films by the screen printing technique," in *Proc. Int. Symp. Microelectron. Conf.*, 1986, pp. 604–609.
- [13] P. K. Ajmera, B. Huner, and H. Rangchi, "On the release of the printing screen from the substrate in the breakaway region," in *Proc. Int. Symp. Microelectron. Conf.*, 1987, pp. 328–334.
- [14] J. A. Owezarek and F. L. Howland, "A study of the off-contact screen printing process—part I: Model of the printing process and some results derived from experiment," *IEEE Trans. Compon., Hybrids Manuf. Technol.*, vol. 13, no. 2, pp. 358–367, Feb. 1990.
- [15] B. Huner, "An analysis of a screen printing system equipped with a trailing blade squeegee," *Int. J. Microcircuits Electron. Packag.*, vol. 16, no. 1, pp. 31–40, 1993.
- [16] G. P. Glinski, C. Bailey, and K. A. Pericleous "A non-newtonian computational fluid dynamics study of the stencil printing process," *J. Mechan. Eng. Sci.*, vol. 215, no. 4, pp. 437–446, Jan. 2001.
- [17] J. A. Anderson, P. C. Claypole, and D. T. Gethin, "Squeegee behavior measurement and modelling for graphics printing," *Res. Technol.*, vol. 4, pp. 17–25, May 1999.
- [18] M. C. Taroni, J. W. Breward, P. D. Howell, J. M. Oliver, and R. J. S. Young, "The screen printing of a power-law fluid," *J. Eng. Math.*, vol. 73, pp. 93–119, Apr. 2012.
- [19] J. Prakash and S. K. Vij, "Load capacity and time-height relations for squeeze films between porous plates," *Int. J. Eng.*, vol. 24, pp. 309–322, May 1973.
- [20] H. Wu, "An analysis of squeeze film between porous rectangular plates," *J. Lubricat. Technol.*, vol. 94, no. 1, pp. 64–68, 1972.
- [21] S. A. Sanni and I. O. Ayomdele, "Hydrodynamic lubrication of a porous slider: Limitations of the simplifying assumption of a small porous facing thickness," *Int. J. Eng.*, vol. 147, no. 5, pp. 1–7, 1991.
- [22] E. Messerschmitt, "Rheological considerations for screen printing inks," *Screen Print.*, vol. 72, no. 10, pp. 62–65, 1982.
- [23] J. Eggers, "Nonlinear dynamics and breakup of free surface flows," *Rev. Modern Phys.*, vol. 69, no. 3, pp. 865–929, 1997.
- [24] D. Hohl, *Screen Printing Technical Foundation*. Fairfax, VA: Private Commun., 1999.
- [25] L. Landau, and B. Levich, "Dragging of a liquid by a moving plate," *ActaPhysicochim.*, vol. 17, no. 3, pp. 42–54, 1942.
- [26] F. P. Bretherton, "The motion of long bubbles in tubes," *J. Fluid Mechan.*, vol. 10, pp. 166–188, Jul. 1961.
- [27] K. J. Ruschak and L. E. Scriven, "Developing flow on a vertical wall," *J. Fluid Mechan.*, vol. 81, pp. 305–316, Jun. 1977.
- [28] K. J. Ruschak, "Boundary flow in a pre-metered device," *Chem. Eng. Sci.*, vol. 31, pp. 1057–1060, Jun. 1976.
- [29] F. Fairbrother and A. E. J. Stubbs, "Relations between acidity and tautomerism," (*Chem. Soc.*, vol. 2, pp. 527–538, May 1935).
- [30] G. I. Taylor, "Cavitation of viscous fluid in a narrow passage," *J. Fluid Mechan.*, vol. 16, no. 4, pp. 595–619, 1963.
- [31] K. J. Ruschak, "The Fluid Mechanics of Coating Flows," Ph.D. thesis, Univ. Minnesota, Minnesota, MN, 1974.
- [32] K. J. Ruschak, "Boundary conditions at a liquid/air interface in lubrication flows," *J. Fluid Mechan.*, vol. 119, pp. 107–120, Jun. 1982.
- [33] J. C. Coyne and H. G. Elrod, "Conditions for rupture of a lubricating film," *J. Lubricant. Tech.*, vol. 92, pp. 4545–4561, May 1970.
- [34] E. D. Dolden, "Fundamental investigations into screen printing," Ph.D. thesis, Univ. Leeds, Leeds, U.K., 2001.



Nikil Kapur received the Ph.D. degree from the School of Mechanical Engineering, University of Leeds, Leeds, U.K., in 1999.

He is a Senior Lecturer with the School of Mechanical Engineering, University of Leeds. His current research interests manufacturing industries including reel-to-reel coating and printing processes.



Steven J. Abbott received the Doctor of Philosophy degree in chemistry from Oxford University, Oxford, U.K., for work carried out at Harvard.

He worked in industry on coating and printing science and became a Research & Technical Director with MacDermid Autotype, Wantage, U.K., after a Post-Doctoral position with the University of Strasbourg. He is now an Independent Consultant with Steven Abbott TCNF and a Visiting Professor with the University of Leeds, Leeds, U.K.



Elisabeth D. Dolden received the Ph.D. degree from the University of Leeds, Leeds, U.K., in 2005, in the area of screen printing, before taking up a position with Sharp Devices of Europe GmbH, Oxford, U.K.

She has worked extensively on design of LCD modules.



Philip H. Gaskell is a Professor of fluid mechanics with the School of Mechanical Engineering, University of Leeds, Leeds, U.K. He was the Head of School from 2001 to 2006. His current research interests include encompass the mathematical modelling of laminar and turbulent flows in general, thin-film coating and reacting flows in particular, together with computational fluid dynamics from both a numerical methods, algorithmic and high performance computing perspective.